J Physiol (2003), **549.1**, *pp.* 121–130
DOI: 10.1113/jphysiol.2003.040857

www.jphysiol.org

Journal of Physiology

Voltage-dependent membrane potential oscillations of rat striatal fast-spiking interneurons

Enrico Bracci*†‡, Diego Centonze†‡, Giorgio Bernardi†‡ and Paolo Calabresi†‡

*Department of Optometry and Neuroscience, UMIST, Manchester M60 1QD, UK, †Clinica Neurologica, Dipartimento di Neuroscienze, Università di Tor Vergata, Rome 00133, Italy and ‡ Fondazione Santa Lucia, IRCCS, Rome 00179, Italy

We used whole-cell recordings to investigate subthreshold membrane potential oscillations and their relationship with intermittent firing in striatal fast-spiking interneurons. During current injections (100–500 pA, 1 s), these cells displayed a highly variable pattern of spike bursts (comprising 1–30 action potentials) interspersed with membrane potential oscillations. The oscillation threshold was −42 ± 10 mV, and coincided with that for action potentials. The oscillation frequency was voltage dependent and ranged between 20 and 100 Hz. Oscillations were unaffected by the calcium channel blockers cadmium and nickel and by blockers of ionotropic glutamate and GABA receptors. Conversely, the sodium channel blocker tetrodotoxin fully abolished the oscillations and the spike bursts. The first spike of a burst appeared to be triggered by an oscillation, since the timing and rate of rise of the membrane potential in the subthreshold voltage region was similar for the two events. Conversely, the second spike (and the subsequent ones) displayed much faster depolarisations in the subthreshold voltage range, indicating that they were generated by a different mechanism. Consistent with these notions, a small pulse of intracellular current delivered during the oscillation was effective in triggering a burst of action potentials that largely outlasted the pulse. We conclude that fast-spiking interneuron oscillations are generated by an intrinsic membrane mechanism that does not require fast synaptic transmission, and which depends on sodium conductance but not calcium conductance, and that such oscillations are responsible for triggering the intermittent spike bursts that are typical of these neurons.

(Resubmitted 4 February 2003; accepted after revision 5 March 2003; first published online 28 March 2003)
Corresponding author P. Calabresi: Clinica Neurologica, Dipartimento di Neuroscienze, Università di Tor Vergata, Via di Tor Vergata 135, Rome 00133, Italy. Email: calabre@uniroma2.it

The striatum is the input station of the basal ganglia, receiving excitatory inputs from many cortical regions, and has motor, cognitive and motivational functions (Bolam *et al.* 2000). Its neuronal population includes medium-sized, spiny GABAergic projection neurons and at least three classes of aspiny interneurons (Kawaguchi *et al.* 1995): (1) large-size 'giant' interneurons that probably correspond to tonically active neurons recorded *in vivo*, have prominent hyperpolarisation-activated inward currents and long-lasting spike afterhyperpolarisations (AHPs), and release acetylcholine (Bennett *et al.* 2000), whose clinical relevance for striatal function has been known for a long time (Spehlmann, 1975); (2) nitric oxide synthase/somatostatin-containing interneurons displaying low-threshold spikes (LTS) and prolonged depolarisations in response to intracellular current injections or synaptic stimulation; these are probably GABAergic (Kubota & Kawaguchi, 2000); (3) parvalbumin-containing fast-spiking (FS) interneurons that have a high maximal firing frequency and short-duration action potentials, and are established as being GABAergic (Kawaguchi, 1993, Kawaguchi *et al.* 1995, Koos & Tepper, 1999, Kubota & Kawaguchi, 2000).

Although projection cells amount to 90–95 % of striatal neurons (Bolam *et al.* 2000), the physiological relevance of striatal interneurons has recently begun to emerge. *In vitro* experiments have shown that acetylcholine and nitric oxide play an essential permissive role in corticostriatal synaptic plasticity (Centonze *et al.* 1999; Calabresi *et al.* 2000). Furthermore, selective ablation of cholinergic interneurons results in severe motor abnormalities *in vivo* (Kaneko *et al.* 2000).

Striatal output is subject to a strong GABAergic control. Striatal projection neurons receive large GABAergic inhibitory postsynaptic potentials (IPSPs) *in vitro* (Koos & Tepper, 1999), and local ejection of GABA antagonists strongly increases the firing rate and the excitability of these cells *in vivo* (Nisenbaum & Berger, 1992).

Several lines of evidence suggest that FS interneurons are mainly responsible for such a GABAergic control. Despite solid anatomical evidence that axon collaterals of projection neurons form synapses in the striatum (Bolam *et al.* 2000), paired recordings have revealed that reciprocal connections between these cells are functionally weak (Jaeger *et al.*

1994; Tunstall *et al.* 2002). Conversely, dual recordings have revealed that action potentials in FS interneurons elicit large-amplitude IPSPs on projection neurons located in their axonal territory (Koos & Tepper, 1999). Since FS interneurons are more numerous than LTS interneurons, they are probably the main source of intrastriatal GABA-ergic inhibition.

We have shown recently that unlike projection neurons, FS interneurons are powerfully excited by dopamine (Bracci *et al.* 2002). Understanding the physiological properties of these cells is therefore important to clarify their role in the striatal circuitry, particularly in relation to feed-forward inhibition (Bolam *et al.* 2000), reciprocal connections with the globus pallidus (Bevan *et al.* 1998) and dopamine action (Calabresi *et al.* 2000; Tang *et al.* 2001).

FS interneurons respond to depolarising current injections with high-frequency, non-accommodating trains of action potentials that cease abruptly and occasionally resume (Kawaguchi, 1993; Koos & Tepper, 2002). The underlying mechanisms are not known. Membrane potential oscillations are visible in published recordings (see for example Fig. 3 of Kawaguchi, 1993 or Fig. 1 of Koos & Tepper, 2002), but they have not been described in detail. The present study investigated the mechanisms underlying these oscillations and their relationship with intermittent firing.

METHODS

Male Wistar rats (postnatal day 20–35) were used, as described previously (Calabresi *et al.* 2000). All procedures conformed to the UK Animals (Scientific Procedures) Act 1986. Briefly, animals were killed under ether anaesthesia, the brain was quickly removed and corticostriatal coronal slices (180–200 μm thick) were cut and maintained at 34 °C in oxygenated solution (composition, mM: 126 NaCl, 2.5 KCl, 1.3 $MgCl_2$, 1.2 NaH_2PO_4, 2.4 $CaCl_2$, 10 glucose and 18 $NaHCO_3$). For recordings, slices were transferred to a submerged chamber and continuously superfused (2–3 ml min^{-1}) at 34 °C; neurons were visualised with differential interference contrast and infrared microscopy (Olympus). FS interneurons were medium-sized cells that could not be visually distinguished from projection neurons. The distinctive electrophysiological properties of FS interneurons, however, allowed their unequivocal identification (see Results). Whole-cell recordings were performed with patch pipettes (2–5 MΩ) filled with intracellular solution containing (mM): 125 potassium gluconate, 10 NaCl, 1 $CaCl_2$, 2 $MgCl_2$, 1 BAPTA, 19 Hepes, 0.3 guanosine triphosphate and 2 Mg-adenosine triphosphate, and adjusted to pH 7.3 with KOH. Whole-cell access resistance was 5–30 MΩ before electronic compensation (60–80 %). Current-clamp recordings were performed in bridge mode with an Axoclamp-2B or an Axopatch 1D amplifier. Input resistance was measured with small (10–50 pA) negative current injections. Drugs were bath-applied at the following concentrations: (+)-MK 801 maleate (MK-801), 30 μM; bicuculline (BMI), 20 μM; 6-cyano-7-nitroquinoxaline-2,3-dione (CNQX), 10 μM; tetrodotoxin (TTX), 1 μM; tetraethylammonium (TEA), 1 mM; $CdCl_2$ 200 μM; $NiCl_2$, 2 mM. When using $CdCl_2$, $NaHPO_4$ was omitted from the external solution to prevent cadmium precipitation.

For the analysis of oscillations and action potentials, the coefficient of variation (CV) for a given measured variable was defined as the ratio between the standard deviation and the average value. The CV was calculated for each neuron individually, considering all quiescent and firing episodes present over at least 10 consecutive current steps (1 s long), and then its average value and standard deviation for a pool of neurons were obtained. Oscillation threshold was defined as the most negative membrane potential level at which spontaneous variation of the membrane potentials, larger than 1 mV in less than 5 ms, took place in both depolarising and hyperpolarising directions. In order to quantify the frequency of an oscillation for a certain neuron, and for a certain experimental condition, only episodes in which at least four consecutive cycles were present, and in which the positive and negative peaks were clearly identifiable, were considered. The cycle period was defined as the interval between two consecutive peaks. Therefore, for each neuron and each experimental condition, this measurement yielded an average period and a standard deviation. Frequency was then calculated as the inverse of the period. Spectral analysis of the oscillations was carried out with a fast Fourier transform (FFT) algorithm (Signal software, version 2.09), using 4096 or 2048 data points (corresponding to 0.4096 or 0.2048 s periods, respectively, as data were acquired at 10 kHz). Unless otherwise stated, all FS interneurons recorded ($n = 32$) were used for analysis. For oscillation analysis, $T_{o\text{-}o}$ was defined as the time interval between the last two consecutive oscillation peaks before a burst of action potentials (Fig. 5*A*). $T_{o\text{-}s}$ was defined as the interval between the last peak before an action potential burst and the time when the membrane potential exceeded the level of the last oscillation peak (Fig. 5*A*). Oscillation slope (expressed in mV ms^{-1}) was defined as the slope of the line connecting an oscillation trough to the next oscillation peak (i.e. as the ratio between the membrane potential difference at these two events and the time elapsed between them). Pre-spike slope was defined as the slope of a line connecting the trough of the last oscillation before a spike burst and the point where the membrane potential exceeded the level of the last oscillation peak (Fig. 5*B*). In each neuron analysed, a comparison between $T_{o\text{-}o}$ and $T_{o\text{-}s}$ and between the oscillation slope and the pre-spike slope was performed by pooling values obtained during several current steps of the same amplitude. In each cell, at least 25 spike bursts (preceded by oscillations) were used for analysis. The histogram of the values of $T_{o\text{-}s}/T_{o\text{-}o}$ and pre-spike slope/oscillation slope (Fig. 5*B*) were obtained by calculating these ratios for each spike burst and then pooling data from different cells.

Values are expressed as mean ± S.D., and statistical comparisons were made using Student's *t* test.

RESULTS

FS interneurons ($n = 32$) were identified based on their typical electrophysiological properties, which were revealed by intracellular current injections (1 s long, ±10–500 pA amplitude) delivered under current-clamp conditions from the resting level (at which the cell was kept without current injection). Neurons were classified as FS interneurons if they had resting membrane potential more negative than −70 mV, maximal firing frequency > 150 Hz (measured on at least three consecutive spikes)

and, when injected with constant positive current, displayed intermittent bursts of action potentials (a burst was defined as a cluster of two or more spikes appearing at > 40 Hz, separated from other spikes by quiescent periods > 200 ms). These properties are distinctive of FS interneurons (Kawaguchi, 1993; Koos & Tepper, 1999, 2002). During action potential bursts, little frequency adaptation was observed (Kawaguchi, 1993). These bursts were abruptly interrupted by quiescent intervals of variable duration, that in turn were interrupted by other bursts of action potentials (examples of this behaviour are illustrated in Figs 1–3). These properties differed markedly from those of other neuronal types that we encountered in the striatal slice, for example projection neurons (which are characterised by strong inward rectification and regular firing; Kita *et al.* 1985; Nisenbaum & Wilson, 1995), LTS interneurons (characterised by prolonged plateau potentials and very high input resistance; Kawaguchi, 1993; Kubota & Kawaguchi, 2000) and LA interneurons (characterised by long-lasting spike AHPs and slow depolarising currents activated by negative current injection; Kawaguchi, 1993, Bennett *et al.* 2000). These differences are illustrated in Fig. 1. The resting membrane potential of FS interneurons was −81 ± 6 mV and their input resistance was 110 ± 28 MΩ. All FS interneurons recorded displayed inward rectification (i.e. negative current steps produced smaller steady polarisations than positive current steps of the same amplitude), although this phenomenon was comparatively less pronounced than in projection neurons (see examples in Fig. 1). A striking feature of FS interneurons was that in contrast to the other neuronal types, their firing pattern during positive current steps was particularly unpredictable. In fact, the duration of the action potential bursts and of the quiescent intervals were extremely variable when the same amount of current was injected repeatedly at the same resting membrane potential. This phenomenon is illustrated in Fig. 2, where the typical firing behaviour of a FS interneuron is compared with that of a projection neuron. In each cells the same step of current was injected repeatedly every 45 s. In the projection neuron, the current steps (400 pA) evoked 8–9 spikes, which started 160–250 ms after the start of the step and then continued regularly at a frequency of 9.4–10.7 Hz, as outlined by the raster plot of Fig. 2*B*. In contrast, in the FS interneuron, while a first action potential was invariably generated at the beginning of each depolarising current step (200 pA), the subsequent spike bursts occurred in an apparently random fashion (see also raster plot of Fig. 2*B*). The variability of FS interneuron firing was assessed quantitatively by measuring the coefficient of variation (i.e. the ratio between standard deviation and average) of spike burst and quiescent period duration (named CV_b and CV_q, respectively). In each FS interneuron, this variability was maximal for a certain amount of suprathreshold injected current (between 150 and 300 pA), while currents larger than 400 pA tended to generate a more stereotyped firing pattern consisting of an initial short burst of spikes followed by a persistent absence of action potentials. For each neuron, the maximal values of CV_b and CV_q for each neuron (i.e. the values calculated as described in the Methods for the current step amplitude that gave rise to the maximal variability) were measured. On average, the maximal CV_b was 89 ± 23 %, and the maximal CV_q was 96 ± 33 %.

The firing behaviour of FS interneurons might have been affected by some slow conductances activated (or inactivated) during the current steps, which may not have fully recovered to resting value when the next step was delivered. However, all of the measured features of the FS interneuron firing pattern did not significantly depend on the interval between applied current pulses in the range 5–60 s.

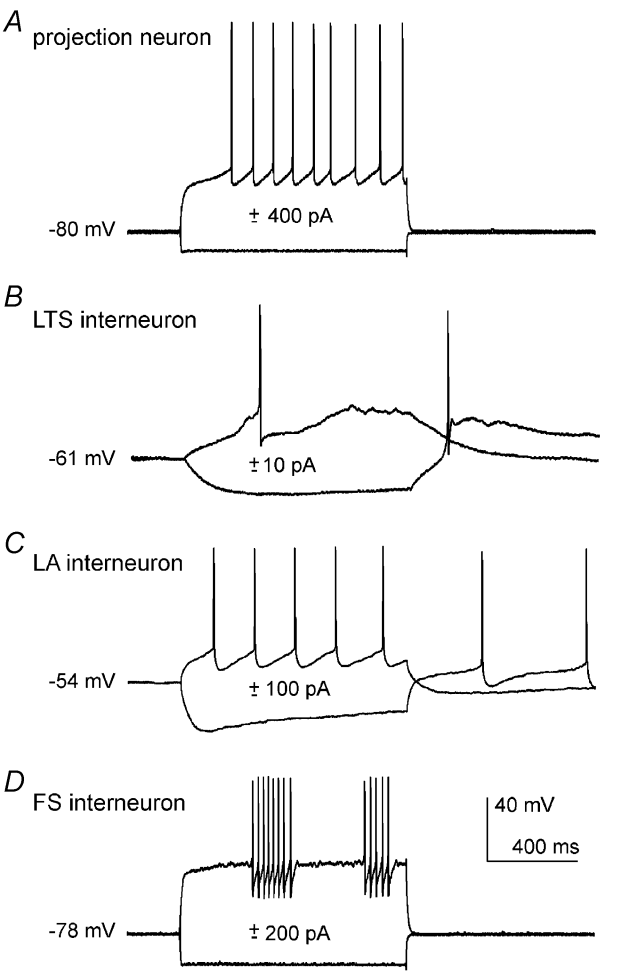

Figure 1. Electrophysiological properties of striatal neuronal types

Intracellular injection of positive and negative current steps revealed different membrane properties in a projection neuron (*A*), a nitric oxide synthase/somatostatin-containing interneuron displaying low-threshold spikes (LTS interneuron, *B*) a large aspiny (LA) cholinergic interneuron (*C*) and a fast-spiking (FS) interneuron (*D*). All cells were recorded without current injection, before and after the steps.

A prominent feature of the quiescent periods between spike bursts was that they were invariably accompanied by subthreshold membrane potential oscillations. The amplitude of these oscillations varied between 1 and 5 mV and they were completely absent at the resting membrane potential (and at more hyperpolarised levels), as illustrated in Fig. 3*A*, *B*. Although oscillation regularity (in terms of period and amplitude) was variable during individual current steps, periods of coherent rhythmicity, in which it was possible to distinguish unambiguously the oscillation peaks, and therefore measure the oscillation period (and frequency), often emerged. Such oscillation appeared only at depolarised potentials, with an average threshold (defined in the Methods) of −42 ± 10 mV. This threshold was not significantly different from that for action potential generation. Oscillations were observed in a voltage range of 8 ± 3 mV above threshold, and disappeared at more depolarised levels, at which trains of action potentials were also absent. In this range, the oscillation frequency was voltage dependent, as illustrated in the example of Fig. 3*C*. This was quantified in 12 neurons in which at least three different membrane potential levels (defined as the average level during the oscillation, as measured by analysis software) differing by > 3 mV were attained with different current pulses. In 10/12 neurons the oscillation period (measured on 15 cycles for each voltage level) was significantly ($P < 0.05$) smaller at the more depolarised level than at the intermediate one, and was significantly ($P < 0.05$) smaller at the intermediate level than at the less depolarised one.

Power spectrum analysis was used to characterise the frequency distribution of the oscillation and, in particular, to reveal whether the irregular appearance of the oscillation was due to a complex spectral composition. FFT of the oscillation episodes (0.4096 or 0.2048 s long, see Methods), however, did not reveal the consistent presence of harmonic components different from the main one. In fact,

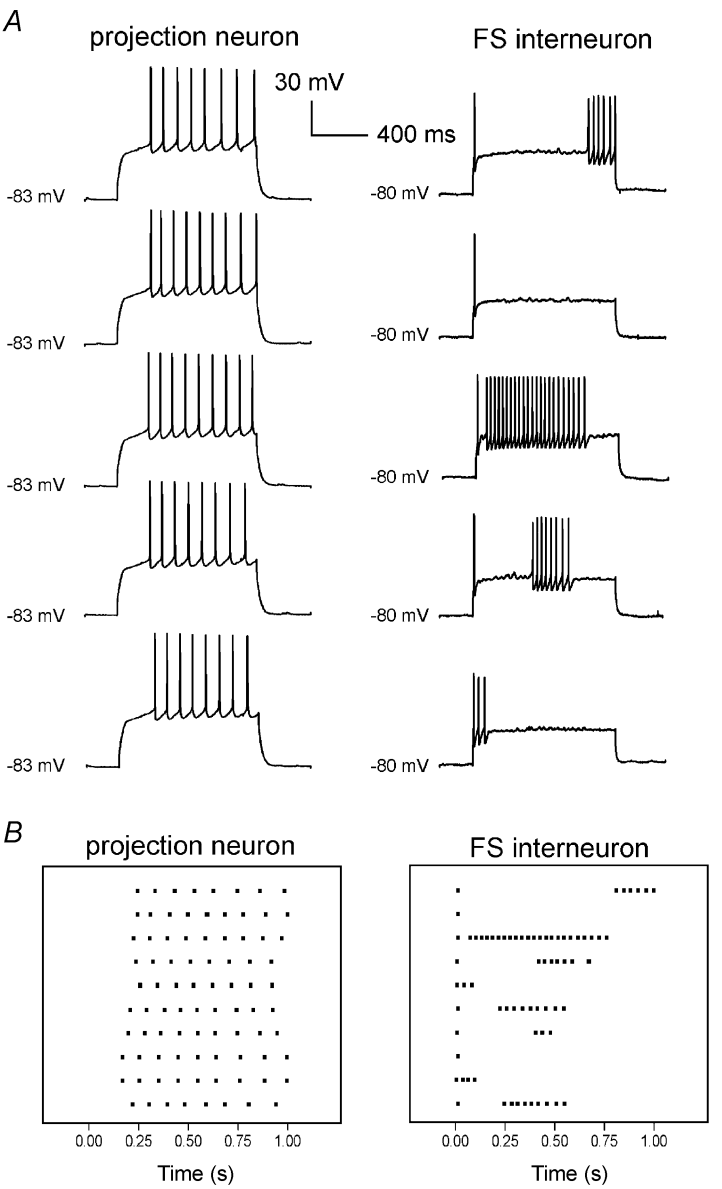

Figure 2. Comparison of firing properties of a projection neuron and a FS interneuron

A, effects on membrane potential of equal steps of current (400 pA for the projection neuron and 200 pA for the FS interneuron) injected every 45 s from the resting level (no current injected). Resting membrane potential was −83 mV for the projection neuron and −80 mV for the FS interneuron. *B*, raster plots (time aligned with traces in *A*) indicating the timing of occurrence of action potentials in the two neurons over 10 consecutive trials (each of which is represented by a horizontal array). The horizontal axis represents time after the start of the depolarising step. Each dot represents an action potential.

averaging the FFTs of > 10 oscillation episodes (recorded consecutively from the same neuron under identical conditions), always produced a power spectrum consisting of a single, roughly bell-shaped, curve centred around the dominant frequency ($n = 12$). A typical example of this behaviour is illustrated in Fig. 4*A*, where the average FFT of oscillations induced in a FS interneuron by 200 pA injections is shown.

Since oscillations and action potentials coexisted during current injections, it was possible to compare their frequency and regularity of occurrence as a function of the injected current. Grouping the experiments carried out on different neurons based on the injected current was preferred to one based on voltage levels, since it was difficult to define the membrane potential level during a spike burst. Frequency of oscillation was not, on average, significantly different from the frequency of spikes occurring during the same current step at 200 pA; however, oscillation frequency was significantly ($P < 0.001$) lower than spike frequency during injections of 300 and 400 pA, as illustrated by the plot of Fig. 4*B*. Maximal oscillation frequency was below 100 Hz in all FS interneurons. The regularity of occurrence of the oscillations for a given amount of injected current was quantified through the CV of their cycle period, measured during those epochs in which it was possible to distinguish oscillation peaks and troughs unambiguously. The coefficient of variation of the cycle period was also measured for the action potentials occurring within each burst during different current steps. As shown in the plot of Fig. 4*C*, the oscillations were significantly ($P < 0.001$) less regular than the action potentials for all current levels tested.

The observation that oscillation frequency was voltage-dependent suggested that this phenomenon is generated

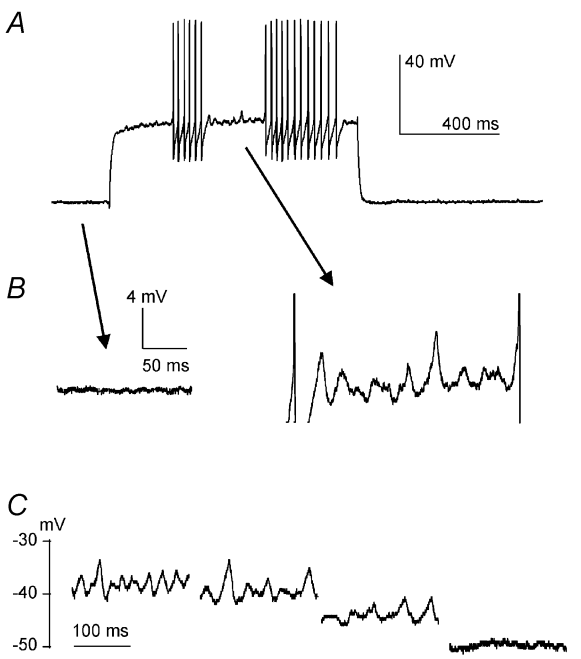

Figure 3. Voltage dependence of membrane potential oscillations in a FS interneuron

In a FS interneuron, positive current injection (300 pA) elicited action potential bursts interspersed with quiescent periods during which membrane potential oscillations were present (*A*). Enlargements in *B* show that these oscillations were absent at the resting membrane potential (−79 mV), but were present when the cell was depolarised by approximately 40 mV. *C*, in the same cell, oscillations appeared when the cell was depolarised by > 33 mV from baseline, and oscillation frequency depended on the level of depolarisation.

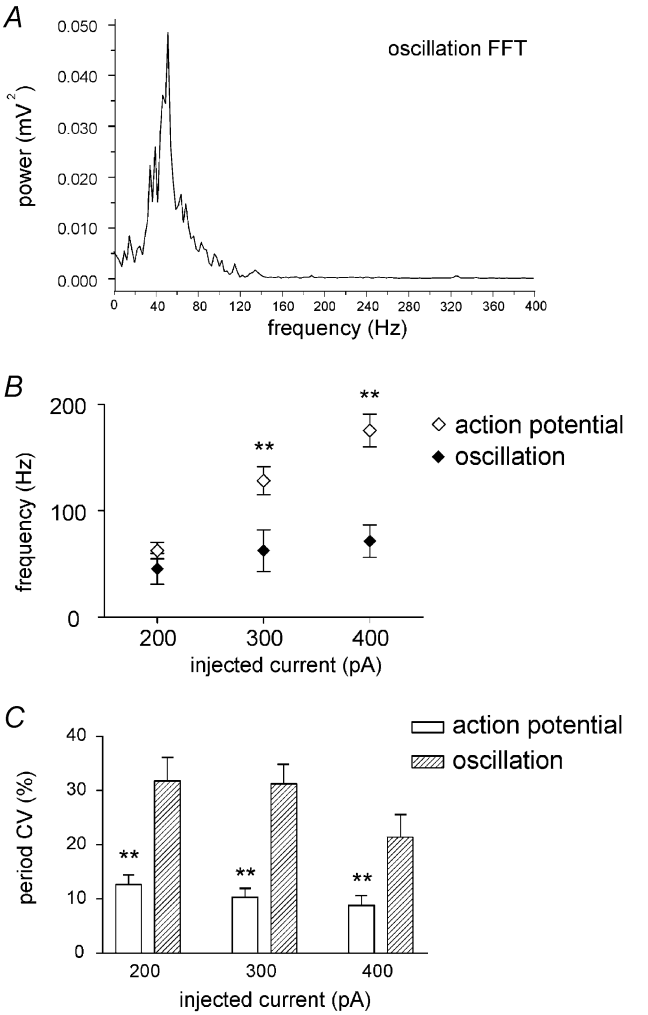

Figure 4. Quantitative features of membrane potential oscillations

A, average fast Fourier transform (FFT) of the oscillations induced in a FS interneuron by 200 pA injections (the average FFT was obtained from individual FFTs of the oscillations elicited by 12 consecutive current injections; 4096 data points). *B*, average dependence of action potential and oscillation frequency on the amount of positive current injected intracellularly. *C*, coefficient of variation (CV) of action potential and oscillation period as a function of the injected current. **Statistically significant difference ($P < 0.001$).

by intrinsic membrane properties of the recorded FS interneuron and was not dependent on the striatal network impinging on it. This was also confirmed by the observation that the oscillations did not depend on fast synaptic excitation or inhibition. In fact, oscillations persisted during co-application of the non-NMDA ionotropic glutamate receptor antagonists CNQX (10 μM), the NMDA ionotropic glutamate receptor antagonist MK801 (10 μM) and the $GABA_A$ receptor antagonist bicuculline (20 μM; $n = 7$), as shown in Fig. 5*A*. On average, in these cells, the period of the oscillations during 200 pA current injections in control solution was 23 ± 8 ms (corresponding to a frequency of 43.5 ± 15 Hz), which is not significantly different from the period in the presence of the antagonists (24 ± 7 ms, corresponding to 42 ± 12 ms). Similarly, the oscillation amplitude was 3.3 ± 1.6 mV in the controls, which is not significantly different from the value of 3.5 ± 1.5 mV recorded in the presence of the antagonists. Spectral analysis failed to reveal the presence of new harmonics in the presence of the antagonists.

In order to test whether the oscillations depended on voltage-dependent calcium conductances, we applied the calcium channel blocker cadmium ($CdCl_2$; 200 μM; $n = 4$) or nickel ($NiCl_2$; 2 mM; $n = 5$), but these agents also failed to significantly affect the amplitude or frequency of the oscillations (Fig. 4*A*) and the intermittent firing properties of fast spiking interneurons.

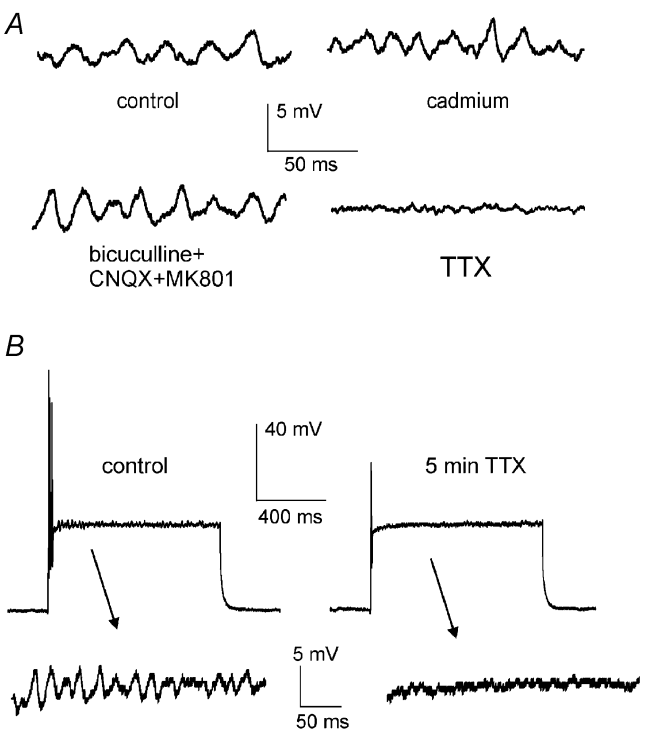

Figure 5. Pharmacology of subthreshold oscillation

A, in a typical experiment on a FS interneuron, voltage-dependent oscillations were not affected by cadmium or by co-application of 20 μM bicuculline, 10 μM CNQX and 30 μM MK801, while they were completely abolished by 1 μM TTX. *B*, in another FS interneuron, the action of 1 μM TTX on the oscillation was complete after 5 min; at the same time a depolarising step elicited only a single, small-amplitude action potential at the beginning of the pulse (this event was fully suppressed 30 s later, not shown).

The possible involvement of calcium-activated potassium currents was further tested with bath application of apamin (Bennett *et al.* 2000; 10 μM; $n = 3$) or by increasing the cytoplasmic calcium chelation by elevating the intracellular concentration of BAPTA (from 1 to 10 mM; $n = 3$; Kuzmiski & MacVicar, 2001). However, these manipulations did not prevent the appearance of the oscillations, and failed to significantly affect oscillation threshold, frequency or amplitude.

On the other hand, the oscillations were fully abolished by the sodium channel blocker TTX (1 μM; $n = 8$), as shown in Fig. 5*A*. The time course of TTX effects on the oscillation was similar to that on somatic spikes; a complete block of the oscillation was observed 4–6 min after TTX application. At this time, action potentials were either fully blocked ($n = 5$), or a single residual action potential with greatly reduced amplitude was still present at the beginning of a depolarising pulse ($n = 3$; Fig. 5*B*) and disappeared soon afterwards. These data showed that voltage-dependent sodium channels (but not calcium channels) were essential for the generation of oscillations.

We then investigated the relationship existing between FS interneuron oscillations and action potential generation. We observed that the first spike of a burst after a quiescent period was almost invariably preceded by oscillations, and that it appeared to be triggered by the depolarising phase of an oscillation occasionally reaching the firing threshold. To test this hypothesis quantitatively, we investigated (1) whether the depolarising membrane potential trajectory that preceded the first spike of a burst had the appropriate phase relationship with the preceding oscillations and (2) if the slope of this depolarisation was similar to that of the rising phase of the other oscillations. To test point (1), we compared the interval between two consecutive oscillation peaks (called $T_{o\text{-}o}$ in the illustrative example of Fig. 6*A*) to the interval between the last oscillation peak and the time when the membrane potential crossed the level of the previous oscillation peak during the depolarisation leading to the first action potential of a burst (termed $T_{o\text{-}s}$ in Fig. 6*A*). As shown by the histogram of Fig. 6*B* (left), the values of $T_{o\text{-}s}/T_{o\text{-}o}$ (measured from 15 FS interneurons, see also Methods) were distributed around unity, as would be expected if the spike was triggered by a large-amplitude oscillation. In each neuron tested, $T_{o\text{-}s}$ did not differ significantly from $T_{o\text{-}o}$ ($P > 0.05$, see Methods). To test point (2), the average slope of the depolarising phase of the oscillations was compared to that of the depolarisation preceding the spike

(Fig. 6*A*, right). Also in this case, the ratio of the oscillation slope to the pre-spike depolarisation slope was distributed around unity (Fig. 6*B*, right), consistent with the idea that the depolarisation leading to the first spike of a burst was of the same nature as the preceding subthreshold ones. In each of 15 FS interneurons tested, the oscillation slope and the pre-spike depolarisation slope did not differ significantly ($P > 0.05$). In order to get temporally more specific information, we also measured (in the same pool of cells) the depolarisation rate during the 5 ms preceding the time when the membrane potential reached the level of the previous oscillation peak during the depolarisation leading to the first action potential of a burst. Again, in this case the values measured did not differ significantly ($P > 0.05$) from those of the subthreshold oscillation preceding the spike burst.

Taken together, these data suggest that the first spike of a burst is in fact triggered by an oscillation, the amplitude of which was large enough to bring the neuron above firing threshold. If this is the case, a small extrinsic current injection at the peak of an oscillation should be able to trigger a spike. To test this hypothesis, we manually injected a small and brief current pulse (10 pA, 5 ms) during oscillations induced by current steps. If the pulse was injected when the membrane potential was less than 1 mV more negative than the spike threshold T (measured independently during spontaneous spike bursts), it was invariably able to trigger a spike burst of variable duration (18 pulses in 3/3 FS interneurons). This phenomenon is illustrated in the example of Fig. 6*C*. On the other hand, in the absence of the current pulse, only 15% of the oscillations crossing the same voltage level (i.e. $T - 1$ mV) triggered a spike burst. The duration of these 'evoked' bursts did not significantly differ from that of spontaneous bursts. Similarly, the CV of evoked burst duration did not significantly differ from that of the spontaneous ones.

Since, as stated above, spike frequency was often higher than oscillation frequency (Fig. 4*B*), it seemed unlikely that the second spike in a burst and the subsequent ones were also triggered by underlying oscillations. This possibility was nonetheless explored by considering the membrane potential trajectory of these spikes within the voltage range

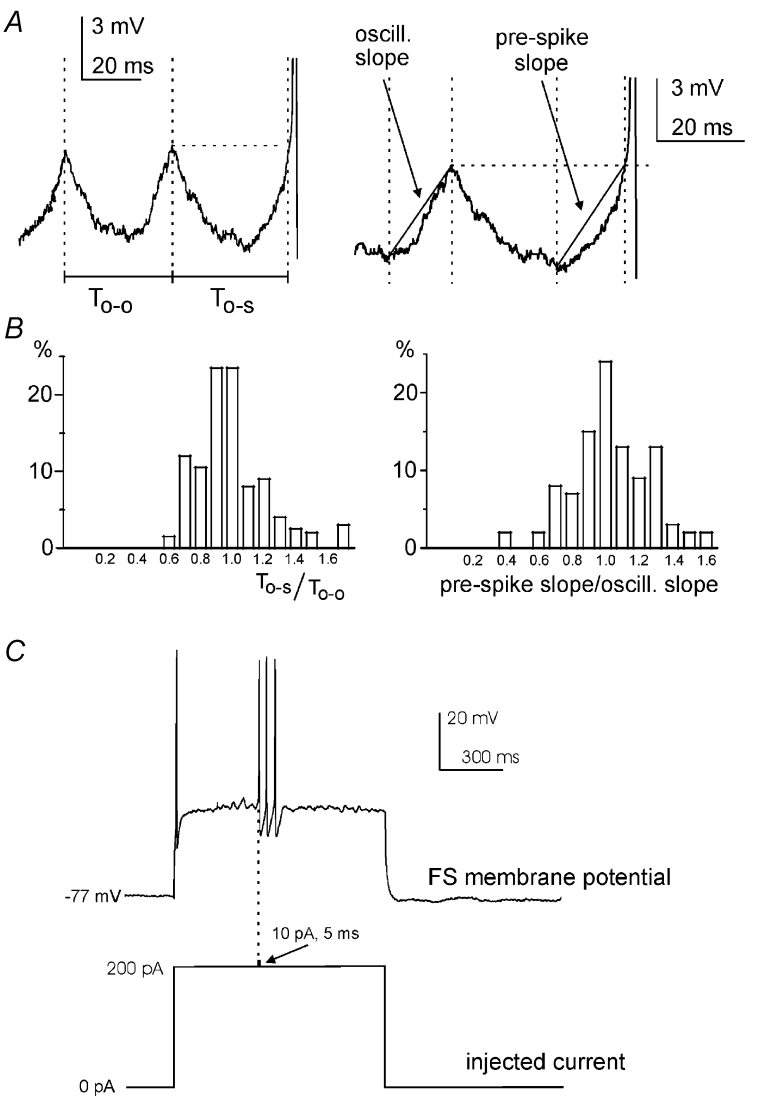

Figure 6. Relationship between oscillations and action potentials

Drawings in *A* illustrate the definition of $T_{o\text{-}o}$ (the time interval between the last two consecutive oscillation peaks before a burst of action potentials), $T_{o\text{-}s}$ (the interval between the last peak before an action potential burst and the time when the membrane potential exceeded the level of the last oscillation peak), oscillation slope (oscill. slope) and pre-spike depolarisation slope (see Methods for details). A case in which the oscillation was particularly symmetric and regular was chosen for this purpose. Histograms in *B* show the distribution of the ratio $T_{o\text{-}s}/T_{o\text{-}o}$ (left) and pre-spike depolarisation slope/oscillation slope (right) in a pool of 15 FS interneurons. *C*, in the experiment illustrated, subthreshold oscillations were elicited by a 200 pA current injection. A small additional current (10 pA, 10 ms) was injected during the rising phase of an oscillation, triggering a train of three action potentials that largely outlasted this current pulse.

typical of the oscillation. Invariably, the depolarising phase of the second spike (and of the following ones) in this voltage range was much faster than that of the first spike. This is illustrated in the example of Fig. 7*A* (left), where the average depolarisation rate in the voltage range of the oscillation is compared for the first (0.6 mV ms^{-1}) and the second (12.8 mV ms^{-1}) spike in a burst. In each cell tested ($n = 15$), the average depolarisation rate of the first spike of a burst was much smaller ($P < 0.001$) than that of the subsequent spikes (on average more than 10 times smaller, as quantified in the plot of Fig. 7*B*). Another difference between the first and the subsequent spikes in a burst was that the first spike was invariably smaller in amplitude than the subsequent ones (on average by 7 ± 2 %, $n = 25$, $P < 0.001$; see examples in Figs 1*D*, 2*A*, 3*A*, 6*C*, 7*A*). These data show that while the first action potential of a burst was triggered by an oscillation of particularly large amplitude, the generation of the subsequent spikes was sustained by a different membrane mechanism.

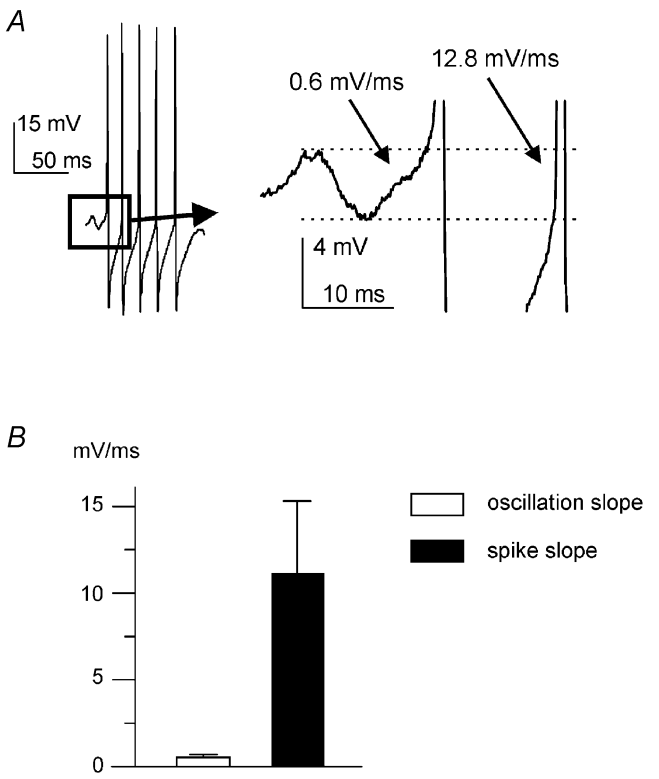

Figure 7. Comparison of subthreshold voltage trajectories for the first and subsequent spikes in a burst

A, in this typical example, the depolarising trajectory in the voltage range in which the oscillations took place is compared for the first spike in a burst and for the subsequent ones in a FS interneuron. The trace on the right is an enlargement of the portion of the left trace enclosed in the box. *B*, plot of the average value of the depolarisation rate for the first spike (open bar) and for the subsequent spikes (black bar).

DISCUSSION

The present data show that striatal FS interneurons subthreshold oscillations are independent of fast synaptic transmission, have a voltage-dependent frequency, require TTX-sensitive sodium conductances and can trigger a burst of action potentials. FS interneurons respond to positive current injections with trains of brief, high-frequency action potentials. These trains have a variable onset time and duration, cease abruptly and then resume after a quiescent interval of variable length. While this behaviour had been described previously in these neurons (Kawaguchi, 1993; Koos & Tepper, 2002), the underlying mechanisms had not been explored. The results of this work show that in FS interneurons, action potential trains are triggered by large-amplitude oscillations, but, once initiated, persist through a membrane mechanism that has faster kinetics than the that responsible for the oscillation.

Neuronal oscillations can either emerge as a result of synaptic interactions in a network, or individual cells can generate them through membrane mechanisms that do not require rhythmic synaptic inputs (Jefferys *et al.* 1996). Several observations suggest that membrane potential oscillations are generated intrinsically by the recorded cell rather than being produced by the neuronal network present in the striatal slice and impinging on FS interneurons. Membrane potential oscillations appeared only when FS interneurons were depolarised beyond approximately −50 mV, and their frequency increased at more depolarised levels. These features are difficult to explain as an emerging property of a network of neurons. Furthermore, the fact that the oscillations were insensitive to co-application of blockers of fast glutamatergic and GABAergic synaptic transmission shows that they were not an emerging property of the striatal network, although GABA and glutamate might play an important role in modulating the oscillation *in vivo*. Therefore, intrinsic ionic membrane mechanisms must be responsible for the oscillations. Calcium conductances were apparently not essential for the generation of the oscillations, since the calcium channel blockers cadmium and nickel failed to affect this phenomenon. Conversely, TTX completely abolished the oscillations, which apparently rely on TTX-sensitive voltage-dependent sodium channels (Novakovic *et al.* 2001). A number of different ionic mechanisms give rise to intrinsic membrane potential oscillations in neurons belonging to different structures. Among these, calcium-independent, TTX-sensitive membrane potential oscillations have been reported in several neuronal types (Klink & Alonso, 1993; Gutfreund *et al.* 1995; Desmaisons *et al.* 1999; Boehmer *et al.* 2000; Wu *et al.* 2001). In particular, the magnocellular neurons of the hypothalamic supraoptic nucleus (Boehmer *et al.* 2000) and trigeminal mesencephalic neurons (Wu *et al.* 2001) display high-

frequency membrane potential oscillations that have been hypothesised to depend on an interplay between TTX-sensitive persistent sodium currents (reviewed by Crill, 1996) and voltage-dependent potassium currents. However, the lack of selective antagonists for the persistent sodium conductance *versus* the rapidly inactivating fast sodium conductance prevented conclusive experiments. In these studies, it has been either explicitly or implicitly assumed that the same membrane compartment giving rise to the action potentials generates the oscillations. It is possible that FS interneuron oscillations depended on a similar mechanism. An alternative explanation is that the subthreshold oscillations recorded somatically reflect action potentials generated in another, more excitable, cellular compartment and are unable to retrogradely invade the soma. In this scenario, the axonal processes would be the most likely source of such action potentials, as in other neurons the axonal compartment (more distal than the axon hillock) is the site of spike initiation when a current is injected into the soma (Colbert & Johnston, 1996). Discrimination between these hypotheses will require the introduction of new selective antagonists for persistent sodium currents, and/or the use of technically challenging axonal and somatic simultaneous recordings.

The present observations also cast light on the mechanisms giving rise to the intermittent, irregular appearance of spike trains in striatal FS interneurons. Whatever their membrane origin, the subthreshold oscillations displayed a marked variability in amplitude. This variability apparently reflected an intrinsically random process, as it did not follow any discernible sequence. When the amplitude of an oscillation was large enough to bring the soma above threshold, a spike train was triggered. This is solidly supported by the fact that the subthreshold trajectory of the depolarisation leading to the first spike of a burst was similar to that of the preceding oscillations. Furthermore, a very small and short current pulse delivered when an oscillation was close to spike threshold was extremely effective in triggering a spike burst that was similar in duration and variability to those that occur spontaneously. Once initiated by an oscillation, the spike train appeared to be able to perpetuate itself by a mechanism different from that which caused the first spike. This is shown by the fact that spikes had a higher frequency than the preceding oscillation, and a much faster rate of depolarisation in the voltage range in which the oscillations took place. The fast, large spike AHP was presumably caused by concomitant fast sodium channel inactivation and potassium channel activation, similarly to other fast spiking neurons (Martina & Jonas, 1997; Martina *et al.* 1998). This AHP presumably reduced the degree of sodium channel inactivation that was present just before a spike burst. Consistent with this notion, the first spike of a burst had always a smaller amplitude than the following ones, although other factors independent of sodium channels may have also contributed to this phenomenon. The fast depolarisation that followed each AHP usually reached the firing threshold, resulting in the generation of the next action potential.

The factors determining the termination of the spike trains remain to be established. Little or no frequency accommodation was observed during spike trains (Kawaguchi, 1993). The termination of the spike train is unlikely to be due to progressive activation (or deactivation) of some ionic conductances. The number of spikes in a train could vary randomly from 1 to 30 despite similar conditions. Although individual ionic channels display a probabilistic behaviour, their collective membrane behaviour is largely deterministic when their number is large (Colquhoun & Hawkes, 1981). The lack of effect of calcium channel blockers on firing behaviour also argues against calcium-activated potassium currents being responsible for spike termination. In the framework of the hypothesis mentioned above, that a distal spike generator was responsible for the oscillations, it is possible to speculate that a negative interference between the somatic and the distal oscillators might have limited the repolarisation following the last spike in a burst, preventing it from reaching threshold.

While technically sophisticated experiments such as axonal recordings may be required to cast light on the factors causing spike train termination, the present results cast light on the peculiar physiological properties of these rarely recorded inhibitory interneurons, which strongly affect the output of the striatum (Koos & Tepper, 1999) and are an important target for the action of dopamine (Bracci *et al.* 2002), the release of which is controlled by another class of GABAergic interneurons in the ventral tegmental area (Johnson & North, 1992). This information will have to be integrated with morphological and electrophysiological data on the connectivity of GABAergic interneurons in order to gain a clearer picture of the local operation of the striatum.

REFERENCES

Bennett BD, Callaway JC & Wilson CJ (2000). Intrinsic membrane properties underlying spontaneous tonic firing in neostriatal cholinergic interneurons. *J Neurosci* **20**, 8493–8503.

Bevan MD, Booth PA, Eaton SA & Bolam JP (1998). Selective innervation of neostriatal interneurons by a subclass of neuron in the globus pallidus of the rat. *J Neurosci* **18**, 9438–9452.

Boehmer G, Greffrath W, Martin E & Hermann S (2000). Subthreshold oscillation of the membrane potential in magnocellular neurones of the rat supraoptic nucleus. *J Physiol* **526**, 115–128.

Bolam JP, Hanley JJ, Booth PA & Bevan MD (2000). Synaptic organisation of the basal ganglia. *J Anat* **196**, 527–542.

Bracci E, Centonze D, Bernardi G & Calabresi P (2002). Dopamine excites fast-spiking interneurons in the striatum. *J Neurophysiol* **87**, 2190–2194.

Calabresi P, Centonze D & Bernardi G (2000). Electrophysiology of dopamine in normal and denervated striatal neurons. *Trends Neurosci* **23**, S57.

Calabresi P, Gubellini P, Centonze D, Picconi B, Bernardi G, Chergui K, Svenningsson P, Fienberg AA & Greengard P (2000). Dopamine and cAMP-regulated phosphoprotein 32 kDa controls both striatal long-term depression and long-term potentiation, opposing forms of synaptic plasticity. *J Neurosci* **20**, 8443–8451.

Centonze D, Gubellini P, Bernardi G & Calabresi P (1999). Permissive role of interneurons in corticostriatal synaptic plasticity. *Brain Res Rev* **31**, 1–5.

Colbert CM & Johnston D (1996). Axonal action-potential initiation and Na^+ channel densities in the soma and axon initial segment of subicular pyramidal neurons. *J Neurosci* **16**, 6676–6686.

Colquhoun D & Hawkes AG (1987). A note on correlations in single ion channel records. *Proc R Soc Lond B Bio Sci* **230**, 15–52.

Crill WE (1996). Persistent sodium current in mammalian central neurons. *Annu Rev Physiol* **58**, 349–362.

Desmaisons D, Vincent JD & Lledo PM (1999). Control of action potential timing by intrinsic subthreshold oscillations in olfactory bulb output neurons. *J Neurosci* **19**, 10727–10737.

Gutfreund Y, Yarom Y & Segev I (1995). Subthreshold oscillations and resonant frequency in guinea-pig cortical neurons: physiology and modelling. *J Physiol* **483**, 621–640.

Jaeger D, Kita H & Wilson CJ (1994). Surround inhibition among projection neurons is weak or nonexistent in the rat neostriatum. *J Neurophysiol* **72**, 2555–2558.

Jefferys JG, Traub RD & Whittington MA (1996). Neuronal networks for induced '40 Hz' rhythms. *Trends Neurosci* **19**, 202–208.

Johnson SW & North RA (1992). Opioids excite dopamine neurons by hyperpolarization of local interneurons. *J Neurosci* **12**, 483–438.

Kaneko S, Hikida T, Watanabe D, Ichinose H, Nagatsu T, Kreitman RJ, Pastan I & Nakanishi S (2000). Synaptic integration mediated by striatal cholinergic interneurons in basal ganglia function. *Science,* **289**, 633–637.

Kawaguchi Y (1993). Physiological, morphological, and histochemical characterization of three classes of interneurons in rat neostriatum. *J Neurosci* **13**, 4908–4923.

Kawaguchi Y, Wilson CJ, Augood SJ & Emson PC (1995). Striatal interneurones: chemical, physiological and morphological characterization. *Trends Neurosci* **18**, 527–535.

Kita H, Kita T & Kitai ST (1985). Active membrane properties of rat neostriatal neurons in an *in vitro* slice preparation. *Exp Brain Res* **60**, 54–62.

Klink R & Alonso A (1993). Ionic mechanisms for the subthreshold oscillations and differential electroresponsiveness of medial entorhinal cortex layer II neurons. *J Neurophysiol* **70**, 144–157.

Koos T & Tepper JM (2002). Dual cholinergic control of fast-spiking interneurons in the neostriatum. *J Neurosci* **22**, 529–535.

Koos T & Tepper JM (1999). Inhibitory control of neostriatal projection neurons by GABAergic interneurons. *Nat Neurosci* **2**, 467–472.

Kubota Y & Kawaguchi Y (2000). Dependence of GABAergic synaptic areas on the interneuron type and target size. *J Neurosci* **20**, 375–386.

Kuzmiski JB & MacVicar BA (2001). Cyclic nucleotide-gated channels contribute to the cholinergic plateau potential in hippocampal CA1 pyramidal neurons. *J Neurosci* **21**, 8707–8714.

Martina M& Jonas P (1997). Functional differences in Na^+ channel gating between fast-spiking interneurons and principal neurones of rat hippocampus. *J Physiol* **505**, 593–603.

Martina M, Schultz JH, Ehmke H, Monyer H & Jonas P (1998). Functional and molecular differences between voltage-gated K^+ channels of fast-spiking interneurons and pyramidal neurons of rat hippocampus. *J Neurosci* **18**, 8111–8125.

Nisenbaum ES & Berger TW (1992). Functionally distinct subpopulations of striatal neurons are differentially regulated by GABAergic and dopaminergic inputs – I. *In vivo* analysis. *Neurosci* **48**, 561–578.

Nisenbaum ES & Wilson CJ (1995). Potassium currents responsible for inward and outward rectification in rat neostriatal spiny projection neurons. *J Neurosci* **15**, 4449–4463.

Novakovic SD, Eglen RM & Hunter JC (2001). Regulation of Na^+ channel distribution in the nervous system. *Trends Neurosci* **24**, 473–478.

Spehlmann R (1975). The effects of acetylcholine and dopamine on the caudate nucleus depleted of biogenic amines. *Brain* **98**, 219–230.

Tang K, Low MJ, Grandy DK & Lovinger DM (2001). Dopamine-dependent synaptic plasticity in striatum during *in vivo* development. *Proc Natl Acad Sci U S A* **98**, 1255–1260.

Tunstall MJ, Oorschot DE, Kean A & Wickens JR (2002). Inhibitory interactions between spiny projection neurons in the rat striatum. *J Neurophysiol* **88**, 1263–1269.

Wu N, Hsiao CF & Chandler SH (2001). Membrane resonance and subthreshold membrane oscillations in mesencephalic V neurons: participants in burst generation. *J Neurosci* **21**, 3729–3739.